ORIGINAL ARTICLE

Asian Herpetological Research 2021, 12(3): 280–288
DOI: 10.16373/j.cnki.ahr.200124

Molecular Evolution of Visual Opsin Genes during the Behavioral Shifts between Different Photic Environments in Geckos

Yao CAI[1,2], Yuefen FAN[1], Youxia YUE[1], Peng LI[1*], Jie YAN[1*] and Kaiya ZHOU[1]

[1] *Jiangsu Key Laboratory for Biodiversity and Biotechnology, College of Life Sciences, Nanjing Normal University, Nanjing 210023, Jiangsu, China*

[2] *School of Food Science, Nanjing Xiaozhuang University, Nanjing 211171, Jiangsu, China*

Abstract Reptiles are the most morphologically and physiologically diverse tetrapods, with the squamates having the most diverse habitats. Lizard is an important model system for understanding the role of visual ecology, phylogeny and behavior on the structure of visual systems. In this study, we compared three opsin genes (*RH2*, *LWS* and *SWS1*) among 49 reptile species to detect positively selected genes as well as amino acid sites. Our results indicated that visual opsin genes have undergone divergent selection pressures in all lizards and *RH2* and *LWS* suffered stronger positive selection than *SWS1*. Twelve positively selected sites were picked out for *RH2* and *LWS*. Moreover, many diagnostic sites were found between geckos and non-gecko lizards, most of which were located near the positively selected sites and some of them have already been reported to be responsible for significant shifts of the wavelength of maximum absorption (λ_{max}). The results indicated that the gecko lineage accelerated the evolution of these genes to adapt to the dim-light environment or nocturnality as well as the switch between nocturnality and diurnality.

Keywords Gecko, diurnality, molecular evolution, nocturnality, opsin gene

[*] Corresponding authors: Dr. Jie YAN, from Nanjing Normal University, China, with her research focusing on taxonomy, systematics and molecular evolution of reptiles; Dr. Peng LI, from Nanjing Normal University, China, with his research focusing on animal ecology and evolutionary biology.
E-mail: yanjie@njnu.edu.cn (Yan J.); lipeng@njnu.edu.cn (Li P.)
Received: 27 September 2020 Accepted: 11 March 2021

1. Introduction

Reptiles are the most morphologically and physiologically diverse tetrapods, which diverged from early tetrapods in the late Carboniferous period approximately 310–320 million years ago along with adaptive evolution (Hughes, 2008). In particular, squamates represent the most diverse radiation of terrestrial vertebrates and occupy ecologically diverse habitat niches. Even though, most of them rely heavily on vision systems as their primary sensory modality which is closely related to the ability and means to interact with their environments (Fleishman *et al*., 2011). Vision in vertebrates is especially well studied, and studies of the evolution of their visual pigments have been able to both identify evolutionary changes, and to ascribe such changes to adaptive evolutionary processes (Hughes, 2008).

The vertebrate retina contains two types of photoreceptor: rods which are responsible for dim light and mediate scotopic vision, and cones acting in daylight, which mediate photopic vision and are necessary with color vision (Bowmaker and Hunt, 2006). Comparative studies across all of the major vertebrates groups have detailed that there are one rod pigment *RH1* (rhodopsin) and four cone pigments encoded by distinct opsin gene families: *LWS*/*MWS* (long/middle-wavelength sensitive opsin gene) maximally sensitive in the red–green spectral region from 490–570 nm, *RH2* (*RH1*-like) sensitive in green from 480–535 nm, *SWS2* (short-wavelength sensitive 2 opsin gene) sensitive in the blue from 410–490 nm and *SWS1* (short-wavelength sensitive 1 opsin gene) sensitive in the violet–ultraviolet from 355–440 nm (Yokoyama *et al*., 2000).

However, different lifestyles were in harmony with different habitat circumstance and various kinds of visual

system. For instance, molecular evidence implies that *LWS* was inactivated on at least five cetaceans which are known to adapt to dim-light field dominated by blue light (Meredith *et al*., 2013). Several groups including cetaceans, pinnipeds, bats, and mole rats, inhabit in low photopic environments, some of which have lost their *SWS1* opsins (Zhao *et al*., 2009). Furthermore, the significant divergent selection in bats *SWS1* and *LWS* was reported to be occurred in response to echolocation ability and foraging habitat, respectively (Gutierrez *et al*., 2018). Among Squamata, dedicated fossorial snakes lost all visual opsins other than *RH1*, whereas all other snakes (including less dedicated burrowers) also have functional *SWS1* and *LWS* opsins. In contrast, all lizards, even highly fossorial amphisbaenians express functional *LWS*, *SWS1*, *SWS2*, and *RH1* genes, and most also express *RH2* (Simões *et al*., 2015).

Lizards provide an important model system for understanding the role of visual ecology, phylogeny and behavior on the structure of visual systems in Squamata (Fleishman and Persons, 2001; Loew *et al*., 2002; Stuart-Fox *et al*., 2007; Macedonia *et al*., 2009). This extensive group includes true chameleons, iguanid lizards, monitor lizards, geckos, and skinks. Some of them are diurnal, and some crepuscular or nocturnal members. Possible changes during transformation of the lifestyle in these reptiles from diurnal to nocturnal have induced some adaptive evolution (Bowmaker, 2008). Therefore, it's notable to explore the evolution of opsin genes owing to lifestyle transformation and understand molecular features and specializations in squamates. For example, *Anolis carolinensis*, a diurnal lizard representive, possesses a complete set of opsin paralogs, however, a nocturnal gecko, *Gekko japonicus* only has three functional opsins: *SWS1*, *LWS*, and *RH2* (Liu *et al*., 2015). This result from genomic sequence data is consistent with the inference of gecko opsin composition based on the wavelength of maximum absorption (λ_{max}) values (Kojima *et al*., 1992, Loew, 1994) and the experiments which failed to detect any hybridizing band using the chameleon *RH1* and *SWS2* cDNA clones as probes in the gecko genome (Shi *et al*., 2001). With the loss of *RH1*, the question of which functional opsin is responsible for nocturnal vision in geckos needs to be solved. The amino acid replacement F89C of *RH2* was suggested to allow geckos to receive more light (Liu *et al*., 2015). However, the evolutionary pattern of opsin they proposed was based on genome data of few species, and more genome data or molecular data from other related species are necessary to determine how particular changes occurred in these opsin genes. In this study, we aimed to further investigate adaptive evolution of gecko opsin genes during their behavior shift between different photic environments by comparing opsin genes among diverse lizard reptiles.

2. Material and Methods

2.1. Taxon Sampling Samples were collected by fieldwork or obtained by academic exchanges. Taxon sampling for surveys of opsin genes comprised 49 reptile species including 40 lizards (ingroups), 6 snakes and 3 turtles (outgroups), 27 of which were newly sequenced and others were downloaded from GenBank in this study (supplementary Table S1). Sample species includes seventeen geckos, six scincoid lizards; eleven Lacertoidea species; one Anguimorpha lizard; five iguanas; and six snakes. Samples used in the molecular analyses are detailed in supplementary Table S1.

PCR and Sequence alignment

Genomic DNA was extracted from muscle tissues of each individual following standard phenol/chloroform extraction methods. We attempted to amplify each exon of *RH2*, *LWS* and *SWS1* visual opsin genes using primers newly designed according to the sequences from *Gekko gecko*, *Phelsuma madagascariensis*, and *Anolis carolinensis* (supplementary Table S2–S4). All fragments were amplified in 50 μL PCR reactions: 1 μL of each primer, 10 μmol/L; 1.8 μL DNA template, ca. 200–300 ng; 5 μL 10 × PCR buffer (Mg^{2+}); 4 μL dNTPs, 2.5 mmol/L; 0.5 μL Takara *Taq* (Takara Biomedical, Dalian, China) and 36.7 μL ddH_2O. The PCR condition was as follows: 3 min at 94°C followed by 35 cycles of 30 s at 94 °C, 30 s at 52–60 °C, 90 s at 72 °C, and a subsequent 10 min final extension step at 72 °C. PCR products were checked by electrophoresis on 1.5% agarose gels and purified with AxyPrep PCR Cleanup Kit (AxyGen MA, USA). Sequencing was carried out bidirectionally on an ABI PRISM 3730 DNA Sequence.

The newly generated sequences were examined by comparison with the published ones by BLAST on NCBI, and then assembled by Lasergene v7.1 (DNASTAR Inc., Madison, WI, USA). After manual editing, all sequences were aligned by MEGA7.0 (Kumar *et al*., 2016). Totally 431 fragments with high-quality were picked and concatenated to 80 opsin genes, and then analyzed together. The newly sequences were deposited in GenBank under accession numbers KU645203-KU645282 (supplementary Table S1).

2.2. Molecular evolution analysis The CODEML program from the PAML 4.9 package (Yang, 2007) was used to estimate the non-synonymous (d_N) and synonymous (d_S) substitution rates and their respective ratio (d_N/d_S or ω) for the *RH2*, *LWS* and *SWS1* genes among squamates. The ω indicates changes in selective pressures, where $\omega = 1$, $\omega < 1$ and $\omega > 1$ corresponds to neutral evolution, purifying and positive selection, respectively. A well-accepted squamate phylogenetic tree was used as a framework tree in our analysis for each gene (Rosler *et al*., 2011, Pyron *et al*., 2013, Zheng and Wiens, 2016). Different datasets, dataset IA (all lizards), dataset IB (all squamates), dataset II (only

geckos), and dataset III (non-gecko lizards) were used for PAML analyses to minimize the effects of sampling.

To examine the probabilities of sites under positive selection in three opsin genes, we used site models M8a (β and $\omega_2 = 1$) versus M8 (Swanson *et al*., 2003; Wong *et al*., 2004) implemented in the CODEML program of PAML 4.9 (Yang, 2007). The nested models were compared using a likelihood ratio test (LRT) with a χ^2 distribution. Positively selected sites in the M8 were identified using a Bayes Empirical Bayes (BEB) analysis (Yang *et al*., 2005) with posterior probabilities ≥ 0.80. Positively selected sites were also detected by fixed effects likelihood (FEL) performed in HYPHY (Pond and Frost, 2005) (via the www.datamonkey.org web server), with the default settings of significance levels of 0.2. We then performed selective pressure detection using TreeSAAP v.3.2 (Woolley *et al*., 2003), which detected selection based on 31 physiochemical amino acid properties. All magnitude category 6–8 changes with $P \leq 0.05$ were used as an index for the degree of radical amino acid substitutions and positive selection.

To evaluate whether positive selection was restricted to specific squamate lineages, we used branch models (including free-ratio model and two-ratio model) (Yang, 1998; Yang and Nielsen, 1998) and branch-site model implemented in CODEML. The free-ratio model (M1) that assumes an independent ω ratio for each branch was compared to the null one-ratio model (M0) with the same ω for all branches (Yang and Nielsen, 1998). Two-ratio model and branch-site model require the foreground branches (lineages tested to be under positive selection) and background branches (rest of the lineages) to be defined a priori. The ω ratios were estimated for two branch categories (geckos as foreground branches versus non-gecko lizards as background branches) in two-ratio model, and then also compared with the null M0 model. The modified branch-site model A with ω varying among sites and among lineages (Zhang *et al*., 2005) was tested against the null hypothesis of no selection in any of the foreground or background branches. Each squamate lineage across the phylogeny was used as the foreground branch, respectively, where the remaining branches were treated as background branches for each gene. A false discovery rate (FDR) correction for multiple tests was applied to the LRT *P* values for branch-site model analysis (Anisimova and Yang, 2007).

2.3. Sliding Window Analyses To explore the further heterogeneous selection pressure at *RH2*, *LWS* and *SWS1* opsin genes across squamate phylogeny, we constructed a sliding window analysis using the program SWAAP (Pride, 2000) with window size at 30 bp and step size at 3 bp, which were repeated for several groups of interest. Sliding window analysis was performed to show variation in ω value (d_N/d_S) along each opsin genes in geckos, non-gecko lizards and all lizards.

2.4. Mapping of positively selected sites onto opsin 3D structures To gain insights into the functional significance of these putatively selected sites, we mapped these positive sites onto protein structures. The 3D structures of opsin genes under positive selection were predicted by using the homology modeling software provided on the I-TASSER server (Zhang, 2008). The protein sequences of positively selected genes were derived from the common Tokay gecko (*Gekko gecko*), which were obtained from the GenBank database.

3. Results

3.1. Visual pigment complement We assembled a dataset of opsin gene sequences for 49 squamates, comprising 17 Gekkota geckos, 6 Scincoidea lizards, 11 Lacertoidea lizards, 1 Anguimorpha lizard, 5 Iguania lizards, 6 Alethinophidia snakes and 3 turtles (outgroups). We have successfully amplified three visual opsin genes (*RH2*, *LWS*, *SWS1*) from genomic DNA of the lizards from 20 families. All sequences were assembled and concatenated correctly for the protein coding region of *RH2*, *LWS*, and *SWS1*, which contain 1065 bp (354 aa), 1110 bp (369 aa), 1044 bp (346 aa), respectively. The sequence alignments had no premature stop codons or frame-shift mutations, which indicated the presence of functional proteins in squamates.

3.2. Selection on opsin genes We found M8 that incorporated selection fitted the data better than the neutral model, M8a, at two opsin genes (*RH2* and *LWS*, $P < 0.05$), suggesting that these genes were subjected to positive selection in squamates. However, for *SWS1*, the LRT showed no significant difference between the models M8 and M8a implying no positive selection. Using M8, the most stringent model carried out in PAML, a small proportion of codons (0.84%–10.17%) were estimated to be under selection with average ω values of 1.292-2.462 at the two positively selected genes in squamates (Table 1). 3 (0.84%), 36 (10.17%), and 3 (0.84%) positively selected sites were identified respectively by the BEB approach as having posterior probabilities ≥ 0.80 at *RH2* in dataset IA (all lizards), dataset II (only gecko), and dataset III (non-gecko lizards). Meanwhile, 6 (1.63%), 7 (1.89%), and 8 (2.17%) positively selected sites were identified respectively at *LWS* in dataset IA, dataset IB (all squamates), and dataset II. However, no positively selected sites were detected at *LWS* in dataset III. When we used a significance threshold of 0.95 for posterior probabilities, the number of positively selected amino acids decreased to two, thirteen, and two for dataset IA, II, and III of *RH2*, while one, one, and two for dataset IA, IB, and II of *LWS*. FEL, performed in HYPHY (Pond and Frost, 2005), was also used to test for selection in the three opsin genes. HYPHY can improve the estimation of the ω value by incorporating variation in d_S whereas d_S is fixed across sequences for all the PAML-based

Table 1 Positively selected sited detected using two maximum likelihood (ML) methods across squamate phylogeny.

Genes	Dataset	Test of selection				Sites under selection identified by ML methods			
		$-Ln$(M8a)	$-Ln$(M8)	$-2\Delta L$	ω value	PAML M8[a]	FEL[b]	No. of sites[c]	% of sites
RH2 (354 aa)	IA: all lizards	8635.191	8629.685	11.012*	2.438	**169**, 209, 213		9	2.54%
	II: only gekkonids	3850.724	3842.002	17.444*	2.111	13, 19, **24**, **39**, 41, 49, 50, 86, 88, 97, 100, 104, 108, **112**, **154**, **158**, 166, 168, **205**, **209**, 210, **213**, 214, 216, 259, 263, 270, 271, 273, 279, 282, 286, 290, 292, 299, 336	**24**, **39**, **112**, **154**, **158**, 162, **169**, **205**, **209**, **213**		
	III: non-gekko lizards	5303.745	5299.837	7.816*	2.462	165, 169, 213			
LWS (369 aa)	IA: all lizards	8911.865	8909.803	4.124*	1.307	**72**, 112, 175, 216, 279, 290	19, **72**, 116, 178, 186, 233, 241, **279**, **290**, 292, 351	3	0.86%
	IB: all squamates	10231.735	10228.664	6.142*	1.292	31, 112, 175, 216, **279**, 282, **290**			
	II: only gekkonids	4165.037	4160.029	10.016*	2.64	31, 112, 175, 182, 188, 229, 279, 282			
	III: non-gekko lizards	5445.293	5444.968	0.65 (NS)	1.585	_		_	_
SWS1 (346 aa)	IA: all lizards	7691.336	7690.724	1.22 (NS)	1.447	_	37, 51, 83, 157, 213, 293	_	_
	IB: all squamates	9505.075	9505.077	0.04 (NS)	1.916	_		_	_
	II: only gekkonids	3324.288	3324.288	0 (NS)	1	_	_	_	_
	III: non-gekko lizards	4752.117	4751.884	0.47 (NS)	1.454	_	_	_	_

The positively selected sites picked out by two methods are shown in bold; * indicates $P < 0.05$ whereas NS indicates 'Not significant'; [a] Codons were detected by M8 model in PAML using a Bayes (BEB) analysis with posterior probabilities ≥ 0.80; [b] Codons were detected by FEL implemented in HYPHY with significance levels of 0.2; [c] No. of sites indicated positively selected sites identified by both ML methods.

analysis. FEL analysis showed that significant signs of positive selection were detected at the three opsin genes with many more positively selection sites than that identified by M8 (Table 1). Combining the two different maximum likelihood (ML) methods, a total of 12 positively selected sites (9 at *RH2* and 3 at *LWS*) were picked out (sites in bold shown in Table 1). Sites that were identified to be under positive selection by two ML methods were regarded as robust candidates for sites under selection. We further employed a complementary protein-level approach implemented in TreeSAAP (Woolley *et al*., 2003) to evaluated destabilizing radical changes at each robust site. The result showed that 10 of 12 sites (83.88%) have at least three radical changes in properties (Table S5, Table S6)

To evaluate whether positive selection is only limited to particular lineages at the three opsin genes, we first used branch models (including free-ratio and two-ratio models) that allow the ω ratio to vary among branches across the phylogeny. The LRT tests showed that relaxation of selective pressure was detected at *RH2* (ω_{geckos} = 0.296, $\omega_{non\text{-}gecko\ lizards}$ = 0.156) and *LWS* genes (ω_{geckos} = 0.398, $\omega_{non\text{-}gecko\ lizards}$ = 0.141; ω_{geckos} = 0.343, $\omega_{other\ squamates}$ = 0.149) when lineage of geckos was treated as foreground branch and the remaining non-gecko lizards or other squamates were treated as background branches. On the contrary, the *SWS1* (ω =0.044) was implied to be under very strong purifying selection (data not shown). Using the stringent branch-site model, we found that ω was greater than 1 at *RH2* in four terminal branches leading to *Cnemaspis limi*, *Phelsuma laticauda*, *Gekko swinhonis*, and *Fylinia* sp. respectively, among which three were nested in the Gekkota clade (Figure 1, Table S5). As well at *LWS*, evidences of positive selection were examined within lineage Gekkota. The ω values were greater than 1 in the last common ancestor (LCA) of Gekkota, terminal branches leading to *Gonatodes annularis*, and leading to *Hemidactylus bowringii* (Figure 1, Table S5). In contrast, in branch-site model significant signs of positive selection were also examined at *SWS1* in some ancestral branches (LCA of Gekkota, LCA of scincids, LCA of lacertids, LCA of *Hemidactylus*, LCA of *Pachydactylus vansoni* + *Phelsuma*) and in one terminal branch leading to *Phelsuma madagascariensis* (Figure 1, Table S5). Furthermore, each identified branch was detected some codons under positive selection. The results of branch-site models suggested more widespread positive selection across opsin genes in geckos than other squamates. This apparent difference can also be observed in the result of our sliding window analyses, with many peaks significantly greater than 1 for geckos, while the curves were uniformly below 1 for the negative control clades with only one exception (Figure 2).

3.3. Spatial distribution of the positively selected residues on opsin 3D structures A total of 12 radical amino acid changes subjected to positive selection identified by two ML methods were mapped onto the 3D structures of two opsin genes (nine at *RH2* and 3 at *LWS*). Opsins are G-protein coupled receptors (GPCRs), which contains seven α-helical transmembrane domains, an extracellular domain, and an intracellular domain to coupled (Terakita, 2005). We found that 11 of the 12 (91.67%) positively selected sites were localized in the α-helical transmembrane domains (supplementary Figure S1).

3.4. Diagnostic amino acid sites between geckos and non-gecko lizards We also compared the amino acid sequences of the three opsin genes between geckos and non-gecko lizards to obtain the information of diagnostic sites. As shown in Table 2, when putting nocturnal and diurnal geckos together, 16 amino acid residues of RH2 differed from those of non-gecko lizards (at residue 40, 41, 42, 43, 49, 50, 54, 56, 60, 64, 83, 85, 98, 285, 289, and 300, on a gray background in Table 2). However, residues 89 and 101 in diurnal geckos represented both status

Table 2 Comparison of the diagnostic amino acid sites between the opsin genes of geckos and non-gecko lizards.

Gene		Codon position																	
RH2		40	41*	42	43	49*	50*	54	56	60	64	83	85	89	98	101	285	289	300
Geckos	nocturnal	L	S/A	F/L	M	V/I/A	V/A	L	G	F	Q	N	L/V	C	S	A	V	T	I/V
	diurnal	L	S/T	F/L	M	I/L	V/I	L	G	F	Q	N	L	C/F	S	A/G	V	T	V
Non-gecko lizards	diurnal	V/I	C	V/C	I	S/F	T	I	I/L/F	L	K	D	F	F	A	G	A	A/S	L

Gene		Codon position					Gene		Codon position							
LWS		220	225	281[a]	298	321	*SWS1*		11	19	56	57	76	85[b]	92[b]	128	149
Geckos	nocturnal	C	L	F	N	Y	Geckos	nocturnal	A	F	A	A	A/V	A	S	L	S/T
	diurnal	C	L	F	H/Y	W		diurnal	A/S/T	F	A	A	A	A/S	S	M	S
Non-gecko lizards	diurnal	V/I	V/I	Y	N	Y	Non-gecko lizards	diurnal	E	W	V	T	T	S	A	F	L/M

* indicates positively selected sites by M8 model in PAML. Underlined sites are reported spectral tuning sites; [a] corresponding to site 277 in Yokoyama and Radlwimmer, 1998; [b] corresponding to sites 90 and 97 in Yokoyama *et al.*, 2006.

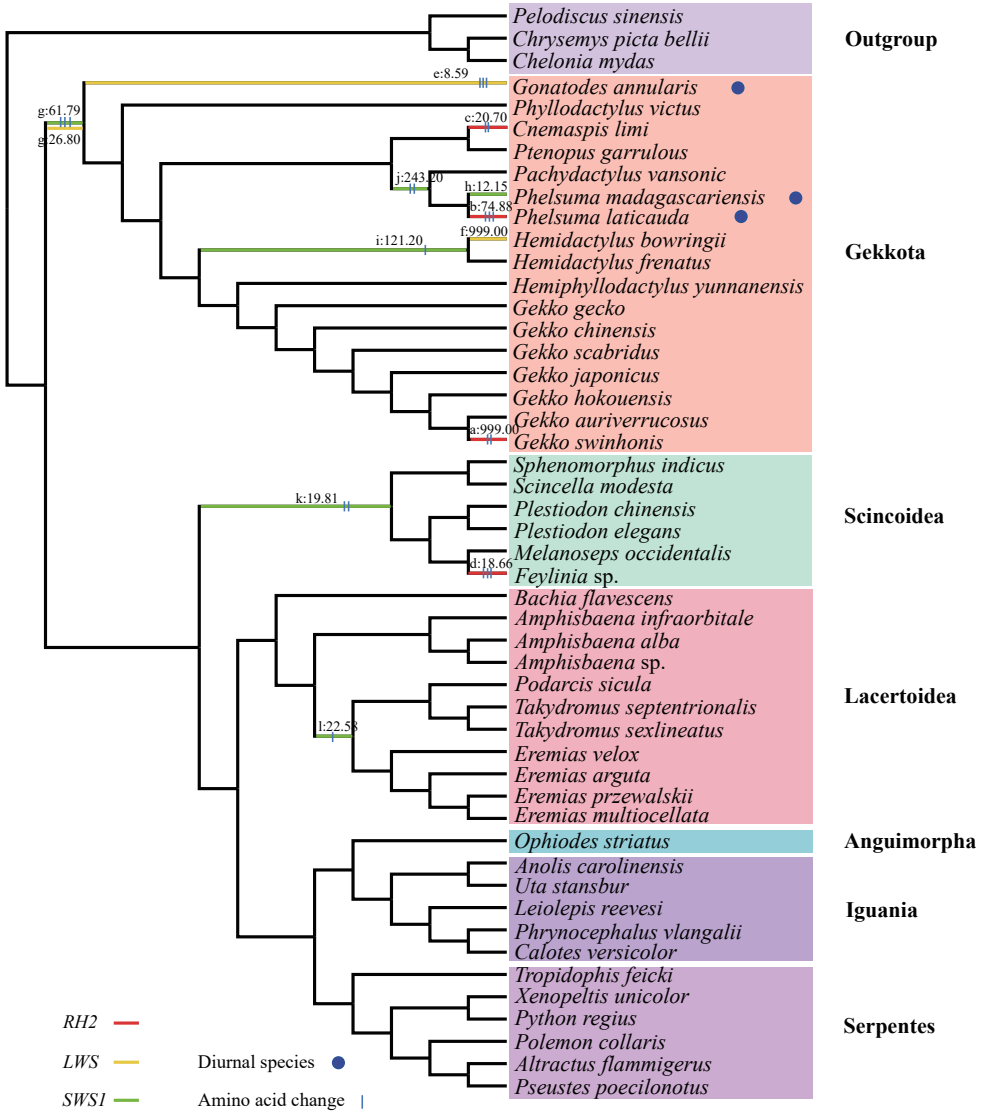

Figure 1 Evidences of positive selection across Squamata phylogeny identified by branch-site model are shown. Three genes are marked with different colors, i.e., *RH2* (red), *LWS* (yellow), and *SWS1* (green). The ω values greater than 1 for individual lineage according to free-ratio and two-ratio are shown. Amino acid changes identified using TreeSAAP across colored branch were indicated by blue vertical lines. The circles were on behalf of diurnal genera in geckos. All detailed results were listed in supplementary Table S5.

found in nocturnal geckos (89C, 101A) and non-gecko lizards (89F, 101G), indicating an intermediate status (shown on a dark blue background). Among all these amino acid residues, three sites (41, 49, and 50, with a star in Table 2) were identified as positively selected sites by M8 model in PAML, and most of the rest are surrounding the positively selected sites. Moreover, certain changes at three sites (49, 83, and 89, underlined in Table 2) have already been reported to cause significant λmax-shifts in various visual pigments during vertebrate evolution (Yokoyama *et al.*, 2007; Takenaka and Yokoyama, 2007). Furthermore, the amino acid in codon position 89 has been reported to be an important functional determinant of rod and cone visual pigments (Yokoyama and Blow, 2001), and the amino acid replacements F89C enables RH2 to have rod pigment-specific biochemical characteristics (Yokoyama and Blow, 2001; Yokoyama and Tada, 2010). F89C was found in all geckos included in this study except one diurnal species (*Gonatodes annularis*). For LWS and SWS1, three and eight diagnostic sites can distinguish geckos and non-gecko lizards, respectively, and one to two sites have been reported to be important spectral tuning sites (Yokoyama and Radlwimmer, 1998; Yokoyama *et al.*, 2006). Among these sites at SWS1, in diurnal geckos both 85A (same to nocturnal gecko) and 85S (same to diurnal lizards) were detected. Besides, two sites which are shared between nocturnal gecko and diurnal lizards (298N and 321Y) were totally different in diurnal geckos (298H/Y and 321W, respectively) (on a light blue background in Table 2).

4. Discussion

Most vertebrates use a combination of rod and cone photoreceptors to enable vision in conditions ranging from starlight to direct sunlight. However, geckos are known to possess a mix of all-rod (nocturnal geckos) or all-cone retinas (diurnal geckos), which are all suggested to be evolutionary derived from cones by both morphological and molecular data (Roll, 2000; Roll, 2001b; Zhang *et al.*, 2006). Based on comparative retinal and photoreceptor morphology, Walls (1942) proposed a scenario for the evolution of photoreceptors in geckos that originated with the loss of rods in a diurnal ancestor of geckos, resulting in an all-cone retina. From this diurnal all-cone state, ancestral geckos transitioned to nocturnality and evolved an all-rod retina through photoreceptor transmutation. Some extant gecko lineages subsequently reverted back to diurnality and re-evolved all-cone retinas through transmutation of the "rods" back into cones (Schott *et al.*, 2019). Recent genome researches provided the evidence of a *RH1* deficiency at the genome level in nocturnal geckos (Hara *et al.*, 2018; Liu *et al.*,

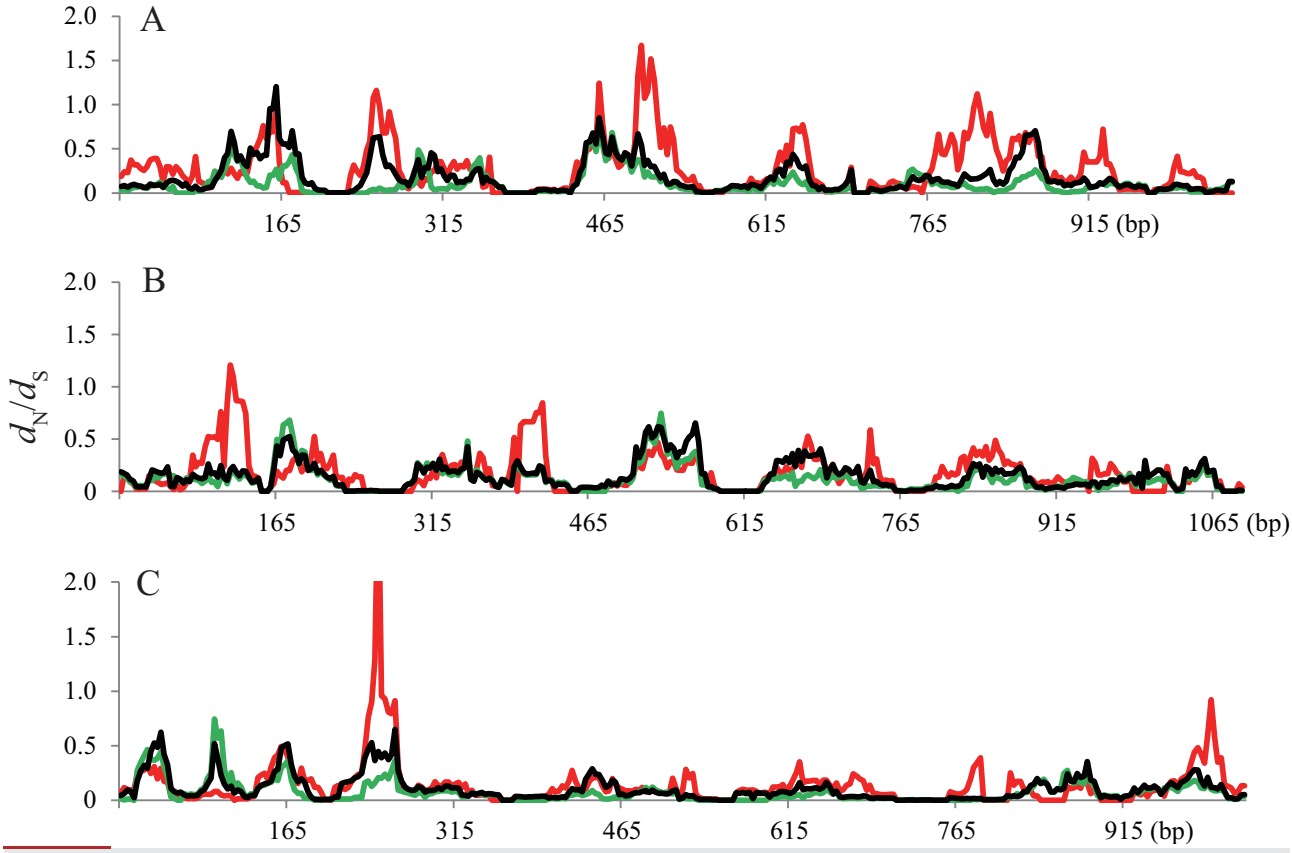

Figure 2 Sliding Window Analyses with window size at 30 bp and step size at 3 bp to show variation in ω value (d_N/d_S) along each opsin genes (A: *RH2*, B: *LWS*, C: *SWS1*) between only geckos (Red), non-gecko lizards (Green) and all lizards (Black).

2015) , and the loss of *RH1* occurred earlier than that of *SWS2*, which was in agreement with the hypothesis that the ancestors of modern geckos were diurnal lizards without rod opsin (Liu *et al*., 2015). Moreover, the F89C amino acid substitution in *RH2* gene shared between the Madagascar ground gecko and Japanese gecko suggested a possible functional switch or compensatory change in cone pigment of geckos that allow them to receive more light (Hara *et al*., 2018; Liu *et al*., 2015). However, the evolution pattern of opsin functional switch was proposed based on genome data of few species. More data from more related species are needed.

As well known, most lizards are strictly diurnal like iguanids, chameleonids, agamids, scincids, lacertids, anguids, pygopodids, and varanids (Roll, 2001a). However, as the largest extant lizard families, most geckos are nocturnal, with some lineages have been reversed back to diurnal. In this study, three opsin genes (*RH1*, *SWS1*, and *LWS*) from nocturnal as well as diurnal geckos, and several lizard species were sampled and analyzed to further investigate the possibly important amino acid changes during evolution or adaptation.

Site models (M8) identified 9 and 3 codons as robust sites under positive selection by at least two Maximum Likelihood methods for *RH2* and *LWS* respectively. However, model M8 failed to identify any positively selected sites for *SWS1* opsin (Table 1), suggesting somewhat purifying selection on *SWS1* opsin gene. In Branch-site model, ω was found to be greater than 1 at *RH2* in four terminal branches, among which three were nested in the Gekkota clade. Similarly at *LWS*, evidences of positive selection were examined within lineage Gekkota (Figure 1). Moreover, significant signs of positive selection were also examined at *SWS1* in some ancestral branches and some codons under positive selection were found which were not supported by the site model. Both of the results of branch-site models and the sliding window analyses supported more positive selection across opsin genes in gecko lineage than in non-gecko lizards.

Among geckos, there are only 15 genera being diurnal (such as *Phelsuma*, *Sphaerodactylus*, and *Gonatodes*) that have pure-cone retinas as a consequence of a change of their habitat (Roll, 2001a). Previous researches revealed difference in anatomical of the retina between nocturnal and diurnal geckos. They pointed that nocturnal geckos had photoreceptors with large rod-shaped outer segments and colored oil droplets in the inner segment whereas diurnal species had much smaller somewhat more cone-like outer segments and colorless oil droplets (Roll, 2000; 2001a). However, our results provided an additional molecular supplement of the opsin genes between nocturnal and diurnal geckos. In all our samples, three species (*Gonatodes annularis, Phelsuma madagascariensis, and Phelsuma laticatus*) on behalf of diurnal genera had undergone stronger adaptive selection than others geckos resulting in transformation of diurnal ambient light (Figure 1). Previous researches have suggested that *RH2* opsin amino acid site 89 is an important functional determinant of rod and cone visual pigments (Shi *et al*., 2001), and the amino acid replacements F89C in geckos enables *RH2* to have rod pigment-specific biochemical characteristics to allow them to receive more light in dim-light environment (Kojima *et al*., 1992; Shi *et al*., 2001; Yokoyama and Tada, 2010; Liu *et al*., 2015; Hara *et al*., 2018). But these researches are based on the comparison of few opsin sequences. In our study, comparing the orthologous *RH2* pigment among 39 species, we deduced that all geckos have amino acid site 89C except *G. annularis* (diurnal) and all non-gecko lizards were 89F (Table 2). 89 F in *G. annularis* is likely to be the result of reversion due to the re-adaptation to daylight. Similar change was also found at site 85 in *SWS1*, which was also a reported spectral tuning site. Furthermore, we also found sites like 298 and 321 in *LWS*, where nocturnal gecko and diurnal lizards share the same residue; however diurnal geckos have different residues. These changes are likely to occur during the evolution of geckos from nocturnality to diurnality.

In conclusion, our results indicate that opsin genes are under different selection pressures in all lizards, and gecko lineage has accelerated the evolution of these genes to adapt to the dim-light environment or nocturnality as well as the switch between nocturnality and diurnality. We compared amino acid sequences of three opsin genes (*RH2, SWS1*, and *LWS*) from representatives of many extant lizard families, which provide clues and evidences for further study of the molecular specialization and evolution to response to different lifestyle (nocturnal or diurnal) in geckos.

Acknowledgements We express special appreciation to B. SUN, Y. LIN and K. GUO for their assistance in sample collection. We are grateful to Y. GUO, K. LI, and Z. WANG for discussions and valuable comments. Financial support was provided by the National Natural Science Foundation of China (NSFC) (Grant No. 31672269 and 31000949 to J. YAN, the Natural Science Foundation of the Jiangsu Higher Education Institutions of China (19KJA330001 to P. LI), the Priority Academic Program Development of Jiangsu Higher Education Institutions (PAPD), and Top-Notch Academic Programs Project of Jiangsu Higher Education Institutions (TAPP, PPZY2015B117).

References

Anisimova M., Yang Z. 2007. Multiple hypothesis testing to detect lineages under positive selection that affects only a few sites. Mol Biol Evol, 24: 1219–1228

Bowmaker J. K. 2008. Evolution of vertebrate visual pigments. Vision Res, 48: 2022–2041

Bowmaker J. K., Hunt D. M. 2006. Evolution of vertebrate visual pigments. Curr Biol, 16: R484–489

Fleishman L. J., Loew E. R., Whiting M. J. 2011. High sensitivity to short wavelengths in a lizard and implications for understanding the evolution of visual systems in lizards. Proc Biol Sci, 278: 2891–2899

Fleishman L. J., Persons M. 2001. The influence of stimulus and background colour on signal visibility in the lizard *Anolis cristatellus*. J Exp Biol, 204: 1559–1575

Gutierrez E. D., Schott R. K., Preston M. W., Loureiro L. O., Lim B. K., Chang B. S. W. 2018. The role of ecological factors in shaping bat cone opsin evolution. P Roy Soc B-Biol Sci, 285: 20172835

Hara Y., Takeuchi M., Kageyama Y., Tatsumi K., Hibi M., Kiyonari H., Kuraku S. 2018. Madagascar ground gecko genome analysis characterizes asymmetric fates of duplicated genes. BMC Biol, 16: 40

Hughes A. L. 2008. The origin of adaptive phenotypes. PNAS, 105: 13193–13194

Kojima D., Okano T., Fukada Y., Shichida Y., Yoshizawa T., Ebrey T. G. 1992. Cone visual pigments are present in gecko rod cells. PNAS, 89: 6841–6845

Kumar S., Stecher G., Tamura K. 2016. MEGA7: Molecular Evolutionary Genetics Analysis Version 7.0 for Bigger Datasets. Mol Biol Evol, 33: 1870–1874

Liu Y., Zhou Q., Wang Y., Luo L., Yang J., Yang L., Liu M., Li Y., Qian T., Zheng Y., Li M., Li J., Gu Y., Han Z., Xu M., Zhu C., Yu B., Yang Y., Ding F., Jiang J., Yang H., Gu X. 2015. *Gekko japonicus* genome reveals evolution of adhesive toe pads and tail regeneration. Nat Commun, 6: 10033

Loew E. R. 1994. A third, ultraviolet-sensitive, visual pigment in the Tokay gecko (*Gekko gecko*). Vision Res, 34: 1427–1431

Loew E. R., Fleishman L. J., Foster R. G., Provencio I. 2002. Visual pigments and oil droplets in diurnal lizards: a comparative study of Caribbean anoles. J Exp Biol, 205: 927–938

Macedonia J. M., Lappin A. K., Loew E. R., Mcguire J. A., Hamilton P. S., Plasman M., Brandt Y., Lemos-Espinal J. A., Kemp D. J. 2009. Conspicuousness of Dickerson's collared lizard (*Crotaphytus dickersonae*) through the eyes of conspecifics and predators. Biol J Linn Soc 97: 749–765

Meredith R. W., Gatesy J., Emerling C. A., York V. M., Springer M. S. 2013. Rod monochromacy and the coevolution of cetacean retinal opsins. PLoS Genet, 9: e1003432

Pond S. L., Frost S. D. 2005. Datamonkey: rapid detection of selective pressure on individual sites of codon alignments. Bioinformatics, 21: 2531–2533

Pride D. T. 2000. SWAAP version 1.0.2, sliding windows alignment analysis program: a tool for analyzing patterns of substitutions and similarity in multiple alignments. Distributed by the author

Pyron R. A., Burbrink F. T., Wiens J. J. 2013. A phylogeny and revised classification of Squamata, including 4161 species of lizards and snakes. BMC Evol Biol, 13: 93

Roll B. 2000. Gecko vision-visual cells, evolution, and ecological constraints. J Neurocytol, 29: 471–484

Roll B. 2001a. Gecko vision-retinal organization, foveae and implications for binocular vision. Vision Res, 41: 2043–2056

Roll B. 2001b. Multiple origin of diurnality in geckos: evidence from eye lens crystallins. Naturwissenschaften, 88: 293–296

Rosler H., Bauer A. M., Heinicke M. P., Greenbaum E., Jackman T., Nguyen T. Q., Ziegler T. 2011. Phylogeny, taxonomy, and zoogeography of the genus *Gekko* Laurenti, 1768 with the revalidation of *G. reevesii* Gray, 1831 (Sauria: Gekkonidae). Zootaxa: 1–50

Schott R. K., Bhattacharyya N., Chang B. S. W. 2019. Evolutionary signatures of photoreceptor transmutation in geckos reveal potential adaptation and convergence with snakes. Evolution, 73: 1958–1971

Shi Y., Radlwimmer F.B., Yokoyama S. 2001. Molecular genetics and the evolution of ultraviolet vision in vertebrates. PNAS, 98: 11731–11736

Simões B. F., Sampaio F. L., Jared C., Antoniazzi M. M., Loew E. R., Bowmaker J. K., Rodriguez A., Hart N. S., Hunt D. M., Partridge J. C., Gower D. J. 2015. Visual system evolution and the nature of the ancestral snake. J Evol Biol, 28: 1309–1320

Stuart-Fox D., Moussalli A., Whiting M. J. 2007. Natural selection on social signals: signal efficacy and the evolution of chameleon display coloration. Am Nat, 170: 916–930

Swanson W. J., Nielsen R., Yang Q. 2003. Pervasive adaptive evolution in mammalian fertilization proteins. Mol Biol Evol, 20: 18–20

Takenaka N., Yokoyama S. 2007. Mechanisms of spectral tuning in the RH2 pigments of Tokay gecko and American chameleon. Gene, 399: 26–32

Terakita A. 2005. The opsins. Genome Biol, 6: 213

Wong W. S., Yang Z., Goldman N., Nielsen, R. 2004. Accuracy and power of statistical methods for detecting adaptive evolution in protein coding sequences and for identifying positively selected sites. Genetics, 168: 1041–1051

Woolley S., Johnson J., Smith M. J., Crandall K. A., McClellan D. A. 2003. TreeSAAP: Selection on Amino Acid properties using phylogenetic trees. Bioinformatics, 19: 671–672

Yang Z. 1998. Likelihood ratio tests for detecting positive selection and application to primate lysozyme evolution. Mol Biol Evol, 15: 568–573

Yang Z. 2007. PAML 4: phylogenetic analysis by maximum likelihood. Mol Biol Evol, 24: 1586–1591

Yang Z., Nielsen R. 1998. Synonymous and nonsynonymous rate variation in nuclear genes of mammals. J Mol Evol, 46: 409–418

Yang Z., Wong W. S., Nielsen R. 2005. Bayes empirical bayes inference of amino acid sites under positive selection. Mol Biol Evol, 22: 1107–1118

Yokoyama S., Blow N. S. 2001. Molecular evolution of the cone visual pigments in the pure rod–retina of the nocturnal gecko, *Gekko gecko*. Gene, 276: 117–125

Yokoyama S., Radlwimmer F. B. 1998. The "five-sites" rule and the evolution of red and green color vision in mammals. Mol Biol Evol, 15: 560–567

Yokoyama S., Radlwimmer F. B., Blow N. S. 2000. Ultraviolet pigments in birds evolved from violet pigments by a single amino acid change. PNAS, 97: 7366–7371

Yokoyama S., Starmer W. T., Takahashi Y., Tada T. 2006. Tertiary structure and spectral tuning of UV and violet pigments in vertebrates. Gene, 365: 95–103

Yokoyama S., Tada T. 2010. Evolutionary dynamics of rhodopsin type 2 opsins in vertebrates. Mol Biol Evol, 27: 133–141

Yokoyama S., Takenaka N., Blow N. 2007. A novel spectral tuning in the short wavelength-sensitive (SWS1 and SWS2) pigments of bluefin killifish (*Lucania goodei*). Gene, 396: 196–202

Zhang J. Z., Nielsen R., Yang Z. H. 2005. Evaluation of an improved branch-site likelihood method for detecting positive selection at the molecular level. Mol Biol Evol, 22: 2472–2479

Zhang X., Wensel T. G., Yuan C. 2006. Tokay gecko photoreceptors achieve rod-like physiology with cone-like proteins. Photochem Photobiol, 82: 1452–1460

Zhang Y. 2008. I-TASSER server for protein 3D structure prediction. BMC Bioinformatics, 9: 40

Zhao H. B., Ru B. H., Teeling E. C., Faulkes C. G., Zhang S. Y., Rossiter S. J. 2009. Rhodopsin molecular evolution in mammals inhabiting low light environments. PLoS One, 4:e8326

Zheng Y. C., Wiens J. J. 2016. Combining phylogenomic and supermatrix approaches, and a time-calibrated phylogeny for squamate reptiles (lizards and snakes) based on 52 genes and 4162 species. Mol Phylogenet Evol, 94: 537–547

Handling Editor: Chen YANG

How to cite this article:

Cai Y., Fan Y. F., Yue Y. X., Li P., Yan J., Zhou K. Y. Molecular Evolution of Visual Opsin Genes during the Behavioral Shifts between Different Photic Environments in Geckos. Asian Herpetol Res, 2021, 12(3): 280–288. DOI: 10.16373/j.cnki.ahr.200124

Appendix

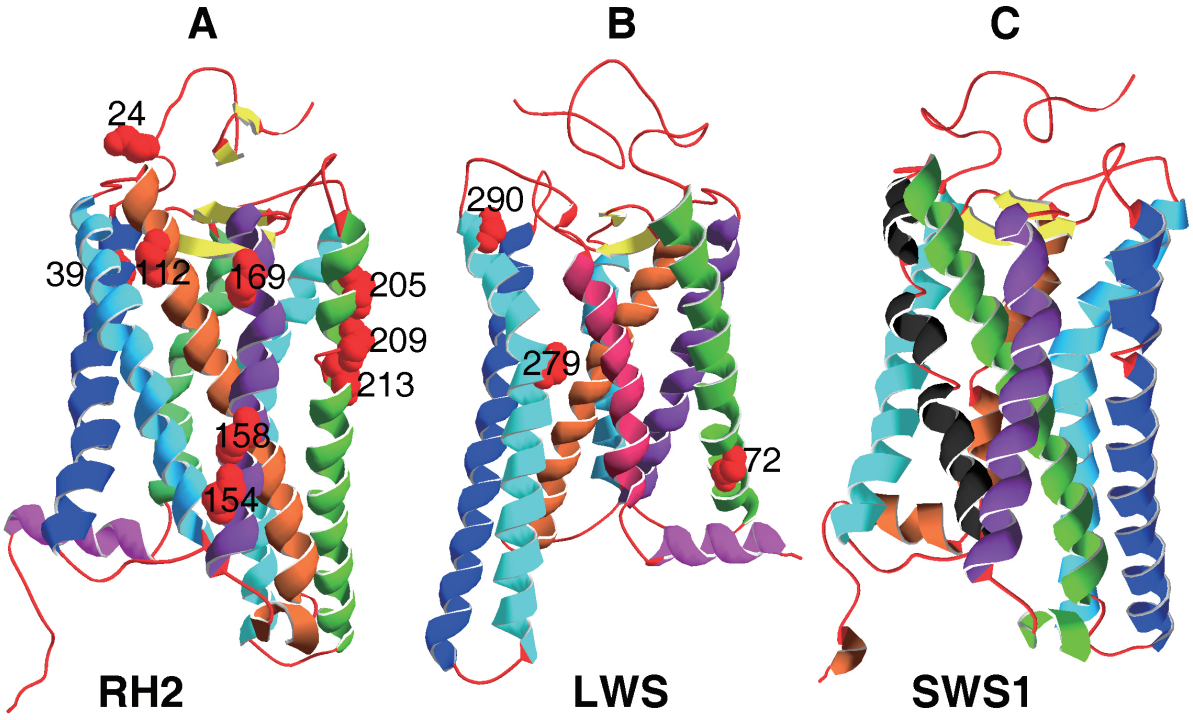

Figure S1 The predicted three dimensional structures (ribbon diagram) of RH2, LWS, and SWS1. α-helices, β-sheets, and loops are represented by spirals, arrows, and lines, and are coloured in different colours, yellow, and red, respectively. A: RH2; B: LWS; C: SWS1. The positive selection sites (24, 39, 112, 154, 158, 169, 205, 209, 213 for RH2; and 72, 279, 290 for LWS) are marked with red globes.

Table S1 Samples with taxon and Genbank accession number. Sequences newly generated for this study are indicated in bold.

Clade/Higher Taxon	Species	Accession Numbers		
		RH2	*LWS*	*SWS1*
Gekkota (17 species)	***Hemiphyllodactylus yunnanensis***	**KU645203**	**KU645230**	**KU645257**
	Hemidactylus bowringii	**KU645204**	**K-U645231**	**KU645258**
	Hemidactylus frenatus	**KU645205**	**KU645232**	**KU645259**
	Gekko auriverrucosus	**KU645206**	**KU645233**	**KU645260**
	Gekko hokouensis	**KU645207**	**KU645234**	**KU645261**
	Gekko scabridus	**KU645208**	**KU645235**	**KU645262**
	Gekko swinhonis	**KU645209**	**KU645236**	**KU645263**
	Gekko japonicus	**KU645210**	**KU645237**	**KU645264**
	Gekko chinensis	**KU645211**	**KU645238**	**KU645265**
	Gekko gecko	M92035	M92036	AY024356
	Phelsuma madagascariensis	AF074044	AF074043	AF074045
	Phelsuma laticauda	**KU645212**	**KU645239**	**KU645266**
	Cnemaspis limi	**KU645213**	**KU645240**	**KU645267**
	Ptenopus garrulous	**KU645214**	**KU645241**	**KU645268**
	Pachydactylus vansonic	**KU645215**	**KU645242**	**KU645269**
	Phyllodactylus victus	**KU645216**	**KU645243**	**KU645270**
	Gonatodes annularis	**KU645217**	**KU645244**	**KU645271**
Scincoidea (6 species)	***Plestiodon chinensis***	**KU645218**	**KU645245**	**KU645272**
	Plestiodon elegans	**KU645219**	**KU645246**	**KU645266**
	Melanoseps occidentalis	KR336743	KR336713	KR336718
	Feylinia sp.	KR336742	KR336714	KR336717
	Sphenomorphus indicus	**KU645220**	**KU645247**	**KU645273**
	Scincella modesta	**KU645221**	**KU645248**	**KU645274**
Lacertoidea (11 species)	*Amphisbaena infraorbi*tale	KR336730	KR336704	KR336719
	Amphisbaena alba	KR336729	KR336705	KR336720
	Amphisbaena sp.	KR336728	KR336706	KR336721
	*Bachia flavescen*s	KR336731	KR336703	KR336715
	Takydromus septentrionalis	**KU645222**	**KU645249**	**KU645275**
	Takydromus sexlineatus	KR336727	KR336707	KR336722
	Podarcis sicula	AY941829	--	--
	Eremias multiocellata	**KU645223**	**KU645250**	**KU645276**
	Eremias velox	**KU645224**	**KU645251**	**KU645277**
	Eremias przewalskii	**KU645225**	**KU645252**	**KU645278**
	Eremias arguta	**KU645226**	**KU645253**	**KU645279**
Anguimorpha	*Ophiodes striatus*	KR336732	KR336708	KR336716
Iguania (5 species)	***Leiolepis reevesi***	**KU645227**	**KU645254**	**KU645280**
	Phrynocephalus vlangalii	**KU645228**	**KU645255**	**KU645281**
	Calotes versicolor	**KU645229**	**KU645256**	**KU645282**
	Anolis carolinensis	**NM001291394**	**U08131**	**XM_003229162**
	Uta stansburana	**DQ100324**	**DQ129869**	**DQ100325**
Serpentes (6 species)	*Tropidophis feick*i	--	KR336709	KR336723
	*Xenopeltis unicol*or	--	FJ497235	FJ497234
	*Python regi*us	--	FJ497238	FJ497237
	Polemon collaris	--	KR336710	KR336724
	*Pseustes poecilonotu*s	--	KR336711	KR336725
	*Atractus flammiger*us	--	KR336712	KR336726
Testudines (3 species)	*Pelodiscus sinens*is	XM_006119345	--	XM_006110204
	*Chrysemys picta bel*lii	XM_005309675	XM_005281282	XM_005281289
	*Chelonia myd*as	XM_007063507	--	XM_007067421

Table S2 Primers for *RH2* exons amplification from genomic DNA.

Exons	Primers	Sequence 5'-3'
Exon1	RH21-F1	5'-ATGAATGGAACAGAAGG-3'
	RH21-R1	5'-CTCCAATTGTTGCAAAGAA-3'
Exon2	RH22-F1	5'-GTCAAGTTGCACTCTGGTC-3'
	RH22-R1	5'-CTGGACCAACCAAACAG-3'
Exon3	RH23-F1	5'-RTWTATACCTGAGGGRATGCA-3'
	RH23-R2	5'-CTCTCGAACTTTGCATATGAG-3'
Exon4	RH24-F1	5'-GCAGCTGCTCAGCARCAGGA-3'
	RH24-R1	5'-CTGTTTGTTCAWGAGGACATA-3'
Exon5	RH25-A1	5'-TTCCGTAAYTGCATGRTCACCA-3'
	RH25-AS1	5'-CTATGCAGGTGMCACTTGGCTGGA-3'

Table S3 Primers for *LWS* exons amplification from genomic DNA.

Exons	Primers	Sequence 5'-3'
Exon1	LWS1-F3	5'-ATGACGGAAGCCTGGAACGT-3'
	LWS1-R1	5'-CCCGGGTGTTGTTGGTGTTGGT-3'
Exon2	LWS2-F1	5'-GCCCTTTCGAWGGTCCAAACTAT-3'
	LWS12-R3	5'-CGCAAGAGGATACGACGTACC-3'
Exon3	LWS3-F2	5'-GTATCACAGGCCTCTGGTC-3'
	LWS3-R2	5'-CTACTCCAGCCAAAGATGGG-3'
Exon4	LWS4-F1	5'-GTACTGGCCYCAYGGTCTGAAGA-3'
	LWS4-R1	5'-CGCACGRATMGCCAMCCACACTTG-3'
Exon5	LWS5-F2	5'-GTNGCYGCCCAGCAGAAAGA-3'
	LWS5-R2	5'-CTGTCTGTTCATGAAGACGTAG-3'
Exon6	LWS6-F1	5'-TTCCGTAACTGCATAWTGC-3'
	LWS6-R2	5'-TTATGCYGGTGATACAGAGGA-3'

Table S4 Primers for *SWS1* exons amplification from genomic DNA.

Exons	Primers	Sequence 5' – 3'
Exon1	SWS11-S21	5'-ATGTCYGGAGAAGAAGACTTC-3'
	SWS11-R2	5'-CTGCTAGGGAGCCGAGGAAGGCCTCCA-3'
Exon2	SWS12-F1	5'-GBCTGGTCACYGGCTGGTC-3'
	SWS12-R1	5'-CTGCTCCACCCGAAAGAGGG-3'
Exon3	SWS13-F1	5'-GTTCATCCCGGAGGGCCT-3'
	SWS13-R2	5'-GGCYCGAAGKGCGCCCAGGAGCTG-3'
Exon4	SWS14-F2	5'-GTAGCCGCYCAGCARCAGGAGT-3'
	SWS14-R1	5'- CTGTTTGTTCATGAAGCA-3'
Exon5	SWS15-F1	5'-TTCCGAGGTTGCATCTTGGA-3'
	SWS15-R1	5'-TTAGCTGGGGCTGACCTG-3'

Table S5 Positive selection detected base on branch-site model in all squamates.

Genes	lineages	Models	-lnL	2ΔlnL	*P* values	ω values	Positively selected sites
RH2	a. *G.swinhonis*	Ma0	8698.916	7.692	0.006	ω0=0.025,ω1=1,ω2=1	137I 0.854, 158A 0.606
		Ma	8695.070			ω0=0.025,ω1=1,ω**2=999.00**	
	b. *P.laticauda*	Ma0	8698.929	4.486	0.034	ω0=0.025,ω1=1,ω2=1	25E 0.855, 108I 0.666, 180P 0.732
		Ma	8696.686			ω0=0.025,ω1=1,ω**2=74.877**	
	c. *C.limi*	Ma0	8696.808	4.466	0.035	ω0=0.024,ω1=1,ω2=1	**199 H 0.991****
		Ma	8694.575			ω0=0.024,ω1=1,ω**2=20.700**	
	d. *F.sp.*	Ma0	8695.962	5.164	0.023	ω0=0.025,ω1=1,ω2=1	**96 Y 0.972***
		Ma	8693.380			ω0=0.025,ω1=1,ω**2=18.660**	
LWS	e. *G.annularis*	Ma0	10298.420	4.65	0.031	ω0=0.03,ω1=1,ω2=1	166I 0.533, 230S 0.731, 275V 0.899, **280A 0.994****, 292V 0.598, 296A 0.775, 298N 0.739, **321Y 0.995****
		Ma	10296.095			ω0=0.03,ω1=1,ω**2=8.593**	
	f. *H.bowringii*	Ma0	10307.880	8.428	0.0037	ω0=0.032,ω1=1,ω2=1	157F 0.817, 166I 0.687, 170S 0.810, 186 A 0.513
		Ma	10303.666			ω0=0.031,ω1=1,ω**2=999.00**	
	g. Gekkota	Ma0	10305.616	4.166	0.041	ω0=0.031,ω1=1,ω2=1	217E 0.654,**220C 0.990****, 281F 0.670
		Ma	10303.533			ω0=0.031,ω1=1,ω**2=26.**797	
SWS1	h. *P.madagascariensis*	Ma0	9721.061	4.984	0.026	ω0=0.034,ω1=1,ω2=1	11A 0.559, 94S 0.660, 179Q 0.945, 208 I 0.535, 223 S 0.602, 258 L 0.909
		Ma	9718.569			ω0=0.034,ω1=1,ω**2=12.145**	
	i. *Hemidactylus*	Ma0	9722.434	8.53	0.0035	ω0=0.035,ω1=1,ω2=1	**15 S 0.998****, 20 D 0.539, 232 Q 0.504
		Ma	9718.169			ω0=0.035,ω1=1,ω**2=121.203**	
	j. *Phelsuma+ P.vansonic*	Ma0	9723.784	10.018	0.0016	ω0=0.035,ω1=1,ω2=1	51 A 0.736, 179 Q 0.719, 258 L 0.703, 322 A 0.801
		Ma	9718.775			ω0=0.035,ω1=1,ω**2=243.195**	
	g. Gekkota	Ma0	9719.132	7.242	0.0071	ω0=0.034,ω1=1,ω2=1	11 A 0.597, **19 F 0.975***, **76 A 0.985***, 128 L 0.500, 149 S 0.873
		Ma	9715.511			ω0=0.034,ω1=1,ω**2=61.788**	
	k. Scincidae	Ma0	9721.746	6.214	0,0127	ω0=0.035,ω1=1,ω2=1	**15 S 0.991****, **37 A 0.973***
		Ma	9718.639			ω0=0.035,ω1=1,ω**2=19.809**	
	l. Lacertinae	Ma0	9721.543	10.052	0.0015	ω0= 0.035,ω1=1,ω2=1	**15S 0.994****, **292S 0.990****
		Ma	9716.517			ω0=0.035,ω1=1,ω**2=22.583**	

Note: Sites with *P* > 0.95 and ω2 >1 are indicated in bold. Any P value higher than 0.99 was designated with two (**) asterisks, and *P* value between 0.95 and 0.99 was designated with one (*) asterisk.

Table S6 Amino acid sites identified as positively selected sites detected using PAML, Datamonkey and TreeSAAP at *RH2*, *LWS* and *SWS1* opsin genes.

Gene	AA[a]	PAML ($P > 0.8$)[b]		Datamonkey[c]			TreeSAAP[d]	
		Site model	Branch-site model	SLAC ($P < 0.2$)	FEL ($P < 0.2$)	REL ($P > 50$)	Amino Acid Properties	AA change
RH2	13	0.827					*hp*	L→H
	19	0.939						
	24	0.872			0.13		*F*	F→Y
							F	Y→F
	25		0.855				*P*	E→D
	39	0.924		0.134	0.043	977.02	$N_s B_r pK' R_a H_p H_t$	I→T
							P_β	V→A
							pK'	I→M
							pK'	I→V
							pK'	V→I
							pK'	I→L
	41	0.853					$P_\alpha P_c P$	S→A
							$N_s B_r \mu$	C→S
	49	0.991				118.56	P_β	V→A
							$R_f P_c F R_a H_t P$	F→S
							$R_f P_c F R_a H_t P$	S→F
							pK'	I→V
							pK'	V→I
	50	0.949					P_α	T→A
							$N_s B_r pK' R_a H_p H_t$	T→I
							P_β	A→V
	86	0.854					P_α	M→T
	88	0.997					$R_f c R_a P$	C→I
	96		0.972				$R_f c E_{sm}$	Y→C
							H_t	Y→T
	97	0.901					P_α	T→A
							P_α	A→T
	100	0.951					pH_t	N→Y
							a_c	Y→H
	104	0.927					*pK'*	V→I
							pK'	I→V
	108	0.947					$N_s B_r pK' R_a H_p H_t$	I→T
							$pK' R_a$	I→A
							pK'	M→I
							pK'	I→M
							pK'	I→V
	112	0.813			0.046		*pK'*	V→I
							pK'	I→V
							pK'	I→L
	137		0.854				*pK'*	I→V
	154	0.807			0.144		*pK'*	I→M
							pK'	M→I
							pK'	L→I
							pK'	I→L
	158	0.952		0.028	0.004	1319.1	$P_\alpha P_c P$	A→G
							$P_\alpha P_c P$	G→A
							$P_\alpha N_s c K^0 pK' a_n$	A→C
							$P_\alpha P_c P$	S→A
							$P_\alpha P_c P$	A→S
							P_α	A→T
							P_β	A→V
	162				0.198	257.8	P_β	V→A

(Continued Table S6)

Gene	AA[a]	PAML ($P > 0.8$)[b]		Datamonkey[c]			TreeSAAP[d]	
		Site model	Branch-site model	SLAC ($P < 0.2$)	FEL ($P < 0.2$)	REL ($P > 50$)	Amino Acid Properties	AA change
	165	0.944					pK'	L→I
	166	0.886					$P_\alpha P_c P$	S→A
							$P_\alpha P_c P$	A→S
							$N_s B_r \mu$	S→C
	168	0.825					$P_\alpha P_c P$	A→G
							$P_\alpha P_c P$	A→ S
	169	0.988		0.153	0.046	630.54	$P_\alpha P_c P$	A→G
							$P_\alpha P_c P$	G→A
							$P_\alpha N_s c K^0 p K' a_n$	A→C
							$P_\alpha N_s c K^0 p K' a_n$	C→A
							$N_s c p K' F \mu$	G→C
							$P_\beta B_l P_c F R_a P$	G→V
	199		0.991				F	H→S
	205	0.983		0.117	0.096	482.93	pK'	I→M
							pK'	V→I
	209	0.996		0.171	0.186	165.95	$N_s B_r p K' R_a H_p H_t$	I→T
							$P_\beta B_l P_c F R_a P$	V→G
							pK'	M→I
							pK'	I→V
							pK'	V→I
							pK'	I→L
	210	0.911					$P_\beta B_l P_c F R_a$	V→G
							pK'	I→M
							pK'	M→I
							pK'	I→V
							pK'	V→I
	213	0.998		0.064	0.033	185.22	$N_s B_r p K' R_a H_p H_t$	I→T
RH2							$N_s R_a$	T→V
							$N_s R_a$	V→T
							pK'	I→M
							pK'	I→V
							pK'	V→I
	214	0.998					$N_s B_r p K' R_a H_p H_t$	I→T
							$N_s R_a$	V→T
							pK'	V→I
							pK'	I→V
	216	0.903						
	251		0.893				$pH_l E_t$	T→K
	259	0.938						
	263	0.953					$R_f c p K' a_n$	L→C
	270	0.94				202.77	$P_\alpha P_c P$	A→G
							P_α	A→T
							$P_\alpha P_c P$	A→S
							P_β	V→A
							pK'	V→I
	271	0.972					P_α	A→T
							$N_s R_a$	T→A
							P_β	V→A
	273	0.912					R_f	F→C
							K^0	F→A
	279	0.822						
	282	0.919					$K^0 P_r p E_t P$	D→A
							P	D→E
							P	E→D
	286	0.989					P_α	T→A

(Continued Table S6)

Gene	AA[a]	PAML ($P > 0.8$)[b]		Datamonkey[c]			TreeSAAP[d]	
		Site model	Branch-site model	SLAC ($P < 0.2$)	FEL ($P < 0.2$)	REL ($P > 50$)	Amino Acid Properties	AA change
RH2							P_α	T→M
							$P_\alpha P_r$	T→E
	290	0.996					pK'	V→I
							pK'	I→V
	292	0.937					$P_\alpha P_c P$	A→S
							P_α	A→T
	299	0.956					$P_\alpha P_c P$	S→A
							$N_s B_t \mu$	S→C
							$N_s B_t \mu$	C→S
	336	0.974						
LWS	19			0.127	0.049		$pK' pH_i M_v M_w H_{nc} V^0 \mu E_{sm} E_t$	R→G
							$pK' pH_i V^0 E_{sm}$	R→S
							E_{sm}	R→H
	31	0.936					pK'	I→M
							pK'	V→I
	59	0.917					pK'	L→I
							pK'	I→L
	63	0.951						
	72	0.819		0.144	0.048		$N_s P_\beta B_t c$	C→T
							$R_f c$	F→C
							$R_f c pK' R_a P$	C→V
							$R_f c pK' R_a P$	V→C
							pK'	V→I
	101	0.894						
	112	0.978					$N_s P_\beta B_t P_c F R_a H_p P$	V→S
							$N_s P_\beta B_t B_t R_f P_c pK' E_t F R_a H_p H_t P$	I→S
							$N_s B_t pK' R_a H_p H_t$	I→T
							$N_s R_a$	V→T
							$N_s R_a$	T→V
							$B_t P_c F R_a P$	V→G
							pK'	V→I
							pK'	I→V
	116				0.198		pK'	I→V
	132	0.974					pK'	I→M
							pK'	M→I
							pK'	I→V
							pK'	I→L
	136	0.836						
	157		0.817					
	170		0.81				$P_\alpha P_c P$	A→G
							$P_\alpha P_c P$	A→S
							$P_\alpha P_c P$	S→A
	175	0.952					$P_\alpha P_c P$	A→G
							$B_t R_f P_c pK' F M_v V^0 R_a H_p H_t P$	I→G
							$B_t P_c F R_a P$	V→G
							$pK' R_a$	I→A
							pK'	I→V
							pK'	L→I
	178			0.04	0.03	320.78	P_β	V→A
							pK'	I→V
							pK'	V→I
							pK'	I→L
	182	0.859					P_β	V→A
							pK'	V→I
							pK'	I→V
	186	0.936		0.135	0.168		$P_\alpha P_c P$	G→A

(Continued Table S6)

Gene	AA[a]	PAML ($P > 0.8$)[b]		Datamonkey[c]			TreeSAAP[d]	
		Site model	Branch-site model	SLAC ($P < 0.2$)	FEL ($P < 0.2$)	REL ($P > 50$)	Amino Acid Properties	AA change
							P_α	T→A
							$P_\alpha P_c P$	A→S
							$P_\beta B_l P_c F R_a H_p P$	V→S
							$P_\beta B_l P_c F R_a P$	V→G
							$P_\beta B_l R_f P_c pK' F M_v V^0 R_a H_p P$	G→I
							$P_\beta B_l P_c F R_a P$	V→G
							P_β	V→A
							P_β	A→V
							pK'	V→I
							R_a	V→T
	188	0.884					$P_\alpha P_c P$	S→A
	216	0.93					$P_\alpha P_t a_c P$	S→E
							$P_\alpha P_c P$	S→A
							$P_\alpha P_c P$	A→S
							$N_s B_t P_c h E_t p R_a H_p E_t P$	V→N
							P_β	A→V
							$K^0 P_r p E_t P$	A→D
							P	D→E
	220		0.99				$R_f c p K' R_a P$	V→C
							pK'	V→I
	229	0.886					$R_f c R_a P$	I→C
							$R_f c R_a P$	V→C
							pK'	I→V
							pK'	V→I
LWS	233			0.164	0.041	116.93	P_β	A→V
							$pK' R_a$	A→I
							pK'	V→I
	241			0.173	0.177		pK'	L→I
							pK'	I→L
	275		0.899				pK'	V→I
	279	0.927			0.18	52.53	P_β	V→A
							pK'	I→M
							pK'	I→V
							pK'	I→L
							pK'	L→I
	280		0.994				$pK' R_a$	A→I
	282	0.981					$R_f c R_a P$	C→I
							$R_f c p K' R_a P$	C→V
	290	0.987		0.009	0.002	132.98	$N_c P_\beta P_c F R_a H_p P$	V→S
							$N_s B_t p K' R_a H_p H_t$	I→T
							$N_s B_t p K' R_a H_p H_t$	T→I
							P_β	V→A
							$R_f P_c F R_a H_t P$	S→F
							$R_f P_c F R_a H_t P$	F→S
							pK'	V→I
	292				0.134		P_β	A→V
	321		0.995					
	351	0. 967			0.016	87.37	P_β	V→A
	15		0.998				E_t	S→K
	19		0.988					
	37		0.973	0.0241	0.035	290.8	P_β	V→A
SWS1							K^0	A→F
							$pK' R_a$	A→I
							pK'	I→V
							pK'	L→I
	51			0.0181	0.0224	376.22	$P_\alpha P_c P$	A→G

(Continued Table S6)

Gene	AA[a]	PAML ($P > 0.8$)[b]		Datamonkey[c]			TreeSAAP[d]	
		Site model	Branch-site model	SLAC ($P < 0.2$)	FEL ($P < 0.2$)	REL ($P > 50$)	Amino Acid Properties	AA change
SWS1							$P_{\alpha}N_sc\mathbf{K^0}pK'a_n$	A→C
							$P_{\alpha}P_cP$	A→S
							P_{α}	A→T
							P_{α}	T→A
							$N_scpK'F\mu$	G→C
							P_{β}	A→V
	76		0.996				P_{β}	A→V
	83			0.0203	0.0774	119.52	$P_{\alpha}P_cP$	A→S
							$N_sP_{\beta}B_tP_cFR_aH_pP$	V→S
							N_sR_u	V→T
							P_{β}	V→A
							pK'	V→I
	149		0.939				$N_sB_tR_fP_cFa_nP$	L→S
	157			0.0898	0.0916	122.09	pK'	V→I
	179		0.945				P_cE_t	Q→G
	194			0.168			$NspHt$	N→Y
							$NspHt$	Y→N
							pHi	K→N
							$FE_{sm}E_t$	H→K
							a_m	Y→H
	213			0.158	0.1418		pK'	L→I
							pK'	I→L
	215			0.0963		83.469	$N_sP_{\beta}B_tR_fP_thE_tF$ $P_tpa_cR_aH_pE_tP$	V→D
							$R_fcpK'R_aP$	V→C
							pK'	I→V
							pK'	V→I
	258		0.909				$N_sB_tpK'R_aH_pH_t$	I→T
							pK'	L→I
	292		0.99					
	293			0.132	0.1184		$P_{\alpha}P_c$	A→S
	322		0.801				P_{α}	T→A

Note: a: Codons identified by both M8 model and FEL were in bold; b: Codons identified by the site model and branch-site model in PAML with $P > 0.8$; c: Posterior probabilities detected in Datamonkey of which SLAC, FEL and REL; d: Amino Acid Properties and AA change were calculated in TreeSAAP.